Loss of placental iron exporter ferroportin causes embryonic demise in late-gestation mouse pregnancy

Chang Cao* and Mark D Fleming

Department of Pathology, Boston Children's Hospital, Boston, MA, USA

* **Corresponding author:** chang.cao@childrens.harvard.edu

Keywords: iron, placenta, syncytiotrophoblast, ferroportin, mouse

Summary statement

SynbCre is a new and efficient transgenic Cre line in the mouse placenta and enables functional validation of the essential role of ferroportin in placental iron transport.

Abstract

Fetal development relies on adequate iron supply by the placenta. The placental syncytiotrophoblasts (SCTB) express high levels of iron transporters including ferroportin1 (*Fpn1*). Whether they are essential in the placenta have not been tested directly, mainly due to the lack of gene manipulation tools in SCTB. Here we aimed to generate a SCTB-specific *Cre* mouse and use it to determine the role of placental *Fpn1.* Using CRISPR/Cas9 technology, we created a *Syncytin b* (*Synb*) *Cre* line (*SynbCre*) targeting the fetal facing SCTB layer in mouse placental labyrinth. *SynbCre* deleted *Fpn1* in late gestation mouse placentas reliably with high efficiency. Embryos without placental *Fpn1* were pale and runted and died before birth. *Fpn1* null placentas had reduced transferrin receptor expression, increased oxidative stress and detoxification responses, and accumulated ferritin in the SCTB instead of the fetal endothelium. In summary, we demonstrate that *SynbCre* is an effective and specific tool to investigate placental gene function *in vivo*. The loss of *Fpn1* in late gestation mouse placenta is embryonically lethal, providing direct evidence for an essential role of *Fpn1* in placental iron transport.

Introduction

The placenta is increasingly recognized as a critical contributor to maternal and fetal health during pregnancy as well as setting the foundation for lifelong well-being. Despite its crucial role in fetal development, the placenta is among the least well-understood organ systems. The importance and paucity of placental research is cited as the driving force for the 2014 launch of the "Human Placenta Project" at the National Institutes of Health, aiming to better understand the role of the placenta in health and disease (Guttmacher, Maddox et al. 2014, Sadovsky, Clifton et al. 2014).

Due to its evolutionary proximity and structural similarity to the human placenta, the mouse placenta has been used to study various aspects of placental development, physiology, and pathology (Roberts, Green et al. 2016, Hemberger, Hanna et al. 2020). The mature mouse placenta consists of three anatomical layers — maternal decidua, junctional zone, and labyrinth— each with distinct function and cell composition (Watson and Cross 2005). The study of global knockout (KO) mice helped identify many essential genes, but it is unclear whether the embryonic phenotype (often lethality) is caused by loss of function in the embryo, the placenta, or both.

Many tools have been developed to target the placenta for gene modification, with the *Cre-LoxP*-based approach being the most cell lineage-specific and more commonly used than cell transplantation and viral infection-based strategies (Renaud, Karim Rumi et al. 2011). There are three commonly used placental *Cre* transgenic lines, driven by different trophoblast-specific genes (Li, Sung et al. 2014). *TpbpaCre* targets a subset of ectoplacental cone-derived trophoblasts including junctional zone spongiotrophoblast, glycogen trophoblasts, and trophoblast giant cells (Calzonetti, Stevenson et al. 1995, Simmons, Fortier et al. 2007). *Cyp19Cre* is pan-trophoblast and is expressed in both labyrinth and spongiotrophoblast layers (Wenzel and Leone 2007). *Gcm1Cre* is the only placental *Cre* that targets the labyrinth syncytiotrophoblasts (SCTB), which function as the metabolic hub at the maternal-fetal interface, in charge of nutrient transport, waste removal, and hormone production. In the *Gcm1Cre* mouse, *Cre* expression is driven by *Gcm1*, an SCTB layer II (SCTBII) transcription factor expressed in early-to-mid-gestation placentas (Nadeau, Guillemette et al. 2009, Nadeau and Charron 2014). However, few publications have used *Gcm1Cre* to study SCTB genes since its generation in 2009, possibly due to its inconsistent and incomplete recombination efficiency (unpublished data, Cao and Fleming).

To address this gap, we used CRISPR/CAS9 technology to generate a SCTB specific *Cre*, driven by *Syncytin b* (*Synb*). *Synb* is a retro-viral envelop gene in SCTBII and is essential for SCTB formation (Dupressoir, Vernochet et al. 2011). Importantly, *Synb* is exclusively expressed in mature placentas after embryonic (E) day 11.5 (Dupressoir, Vernochet et al. 2011), making the *Cre* particularly useful to study gene functions in late gestation placentas.

To demonstrate its effectiveness, we used *SynbCre* to study the physiological role of placental iron exporter *Fpn1*. *Fpn1* is the only known mammalian non-heme iron exporter and is critical for iron efflux in high iron trafficking cells including duodenal enterocytes, iron-recycling macrophages, and hepatocytes (Nemeth and Ganz 2021). *Fpn1* is an ideal gene to interrogate with *SynbCre*. First, *Fpn1* is among the most highly expressed genes involved in iron transport and metabolism in the mouse placenta (Cao, Prado et al. 2021), and its protein is expressed in SCTBII, that also exclusively expresses *Synb* (Cao and Fleming 2021). Second, the current knowledge of placental *Fpn1* function is largely deduced from studies in whole-body *Fpn1* KO (Donovan, Lima et al. 2005) and hypomorphs (Mok, Mendoza et al. 2004) that have significant limitations. For example, it is unclear whether embryonic anemia in *Fpn1* hypomorphic mutants is due to the absence of *Fpn1* in the embryo, the placenta, or both. Furthermore, *Fpn1* KO embryos die before the maturation of the placenta, thus precluding any conclusions regarding placental *Fpn1*. Deletion of *Fpn1* in the SCTBII is needed to unequivocally study its role in placental iron transport.

We hypothesized that loss of placental *Fpn1* will cause iron deficiency in the embryo as well as compensatory upregulation of other genes involved in iron transport in the placenta. However, these changes will not meet the high fetal iron demand in late gestation and embryonic death will ensue.

Results and Discussion

SynbCre is expressed in late gestation placentas and is specific to SCTBII

Of the 98 pups born from CRISPR microinjections, 33 (21 males and 12 females) had correct *Cre* targeting as indicated by PCR amplicons of expected size at both insertion junctions (Fig. 1A). The *Cre* transgene was inherited at the expected ratios in both male and female offspring.

To localize *SynbCre* expression in the placenta, *SynbCre* was crossed to a reporter line containing a Yellow Fluorescent Protein (YFP) gene downstream of a floxed STOP sequence (Fig. 1B). *Cre*-induced removal of the STOP sequence and subsequent YFP expression was

detected in the SCTBII of the *Cre*-positive placenta. Cre-negative placentas did not express YFP. These data confirm the specificity of *SynbCre* expression and recombination efficiency in the SCTBII.

Next, we determined the time course of *SynbCre* after mid-gestation (Fig. 1C). Transcript abundance of *Cre* transgene rose sharply at E12.5 and remained elevated throughout pregnancy. In addition, *Cre* was highly correlated with *Synb* mRNA expression (Fig. 1D), consistent with our design of using *Synb* to drive *Cre* expression. *Cre* was not detected in any adult or fetal tissues analyzed (Fig. 1E), a pattern that mirrors the placental exclusivity of *Synb* (Dupressoir, Vernochet et al. 2011).

***SynbCre* is effective at deleting *Fpn1* in the mouse placenta**

To demonstrate the utility of the *SynbCre* line, we crossed the line to mice carrying a conditional allele of *Fpn1*. *SynbCre*-mediated deletion of the *Fpn1* floxed allele was confirmed by the appearance of the *Fpn1 KO* allele in $Fpn1^{fl/+}$ placentas carrying *SynbCre* (Fig. 2A). Placental *Fpn1* KO (pKO) was generated by crossing homozygous *Fpn1 floxed* females with males carrying *SynbCre* harboring a heterozygous *Fpn1 KO* allele. No viable pKO pups were observed at birth (n=29 pups from 4 litters, Chi-square test P = 0.02). A pale and small phenotype was consistently observed in pKO embryos after E15.5 (Fig. 2B). The crown-rump length of the pKO embryos at E15.5 was on average 11.3% shorter than the control embryos (12.6 ± 0.7 mm vs. 14.2 ± 1.0 mm, P = 0.0006).

Compared to the controls, pKO embryos had elevated liver transferrin receptor (*Tfrc*) mRNA (P = 0.01) and non-significantly lower *Hamp* mRNA (P = 0.13) (Fig.S1). Liver iron staining in the pKO embryo was also less intense than the control (Fig.S1). This mild iron deficiency phenotype echoes the observation in late gestation *Fpn1* hypomorph embryos (Mok, Mendoza et al. 2004). Placental size as measured by placental disk diameter did not differ between pKO and control placentas (7.6 ± 0.3 mm vs. 7.5 ± 0.4 mm, P = 0.6). In addition, like the *Fpn1* hypomorph placentas (Mok, Mendoza et al. 2004), there were no obvious structural abnormalities in the pKO placental labyrinth (Fig. 2C). This may be consistent with *Fpn1*'s sole function as an iron transporter with no direct involvement in cellular pathways that have multifaceted and/or systemic effects.

We verified *Fpn1* deletion in the pKO placenta at the mRNA and protein levels. Despite relatively high variation in *Cre* expression among placentas, the degree of *Fpn1* deletion was comparable in all pKO placentas compared to the *Cre* negative littermate placentas. This indicates a threshold effect of *SynbCre* mediated recombination of the *Fpn1 floxed* allele and

the efficiency of Cre mediated recombination needs to be empirically validated when used with other floxed genes. Using quantitative PCR (qPCR) primers that target one of the two deleted *Fpn1* exons, we showed that the *Fpn1* transcript level was 50% lower in pKO placentas than in the controls (Fig. 2D). The residual *Fpn1* transcript expression in the pKO placenta is likely derived from macrophages and other types of trophoblasts not targeted by the *Cre.* Exon usage analysis of the RNA-sequencing data showed that pKO placentas had significantly fewer reads from the two deleted *Fpn1* exons (Fig. S2). Remarkably, there was a 90% reduction of FPN1 protein in pKO placentas compared to the controls (Fig. 2E). Immunofluorescence demonstrated a near-complete absence of FPN1 in the SCTBII of pKO, which displayed normal FPN1 in the fetal liver (Fig. 2F). This confirms that the anemic phenotype of pKO embryos is a direct consequence of *Fpn1* deletion in the placenta, not in the embryo. Using the epiblast specific *Meox2 Cre*, Donovan et al. (Donovan, Lima et al. 2005) showed that embryos with *Fpn1* deletion were viable and attributed their survival to the preservation of *Fpn1* expression in the placenta. Here, the lethality of embryos lacking placental *Fpn1* directly demonstrate an essential role of placental *Fpn1* in supporting fetal growth in late gestation.

In addition to FPN1, *transferrin receptor* (*Tfrc)*, the key cellular iron importer, was reduced by 70% in pKO placentas (Fig. 2E). Immunofluorescence localized the TFRC downregulation to the SCTB layer I (SCTBI) (Fig. 2G). Thus, the mild iron deficiency in the pKO embryos was likely a consequence of the combined deficiencies of the two primary placental iron transporters, TFRC and FPN1.

pKO placenta accumulates ferritin in SCTB

Because *Fpn1* is an iron exporter, we hypothesized that loss of *Fpn1* would block iron export and cause iron accumulation inside the SCTB. To examine iron distribution in the placental layers, we performed diaminobenzidine tetrahydrochloride (DAB)-enhanced Perl's iron stain in pKO and control placentas. There was no stainable iron in the SCTB of either genotype (Fig. S1). In our experience, it is common for the labyrinth to have little stainable iron, even with DAB enhancement to increase signal sensitivity. The relatively low storage iron in the labyrinth may reflect its transit role in iron transfer and the potential toxicity of high intracellular iron. Consistent with the iron staining results, non-heme iron concentrations did not differ between pKO and control placentas (18.8 ± 13.3 vs. 16.1 ± 15.1 μg/g, P = 0.6).

Thus, we explored using ferritin immunofluorescence as an alternative to determine iron distribution in the labyrinth layers (Fig. 2H). In the control placenta, most ferritin was localized in the fetal endothelium and SCTBII, with little staining in the SCTBI. In the pKO placenta, ferritin

was found in both SCTB layers and was nearly absent from the fetal endothelium. The shift of ferritin storage from fetal endothelium to SCTB in the pKO supports the hypothesis that *Fpn1* is needed for iron export from SCTB to the fetal circulation as illustrated in Fig. 2I.

pKO placenta has increased oxidative stress response and detoxification genes

RNA-sequencing identified 12 down-regulated and 36 up-regulated differentially expressed genes (DEGs) with greater than 1.5-fold-change in the pKO placentas compared to the controls (Fig. 2J). *Tfrc* transcript expression was 74% lower in the pKO placentas compared to the controls, consistent with marked reductions of TFRC protein in the pKO placentas shown by western blot (Fig. 2E) and immunofluorescence (Fig. 2G). Because *Tfrc* mediates the primary route of placental iron uptake, its downregulation may be a very effective and compensatory response to prevent iron accumulation and its associated toxicity in the pKO placenta. We have previously shown that *Tfrc* expression in mouse placentas is a reflection of both a programmed/temporal control by gestational age as well as an acute/localized regulation by intracellular iron levels (Cao, Prado et al. 2021). We and others have shown that placental *Tfrc* regulation by iron alone is of low magnitude (Cao, Prado et al. 2021, Sangkhae, Fisher et al. 2021). Thus, the high degree of *Tfrc* downregulation in the pKO placenta is likely an accumulated effect of early and sustained suppression by subtle changes in intracellular iron caused by *Fpn1* deletion.

None of the other putative placental iron transporter genes, including *Slc11a2* (Gunshin, Fujiwara et al. 2005) and *Slc39a8* (Gálvez-Peralta, He et al. 2012), were significantly different in the pKO placentas. Expression of erythroid differentiation genes — including ferrochelatase (*Fech*), 2,3-bisphosphoglycerate mutase (*Bpgm*), and tripartite motif-containing 10 (*Trim10*) — were also lower in pKO placentas. This may indicate lower erythropoietic activity of the nucleated fetal red blood cells in pKO placentas.

On the other hand, genes involved in oxidative stress response and detoxification such as NAD(P)H dehydrogenase, quinone 1 (*Nqo1*), peroxiredoxin 6 (*Prdx6*), catalase (*Cat*), and glutathione S-transferase, alpha 3 (*Gsta3*), were upregulated in the pKO placenta (Fig. 2K). Complete lists of DEGs and gene ontology (GO) enrichment pathways are provided in Table 2S and 3S. qPCR analysis of selected iron transport and oxidative stress genes in the pKO and control placentas is shown in Fig. S3.

Activation of the oxidative stress response and hydrogen peroxide catabolic pathway in the pKO placentas may be a direct result of increased free intracellular iron in the SCTB, as paralleled by its ferritin accumulation (Fig. 2H). However, the increase in free iron was likely mild

because there was no significant iron accumulation in pKO placentas as indicated by iron stain and ferritin western blot. In addition, elevations of oxidative stress processes were moderate and limited to a few genes in the pathways. Thus, gene expression in pKO placentas likely captured the initial and sensitive transcriptomic response to mild increases in intracellular free iron and its associated oxidative stress.

A major challenge in placental research has been the inability to manipulate genes specifically in the placenta without affecting other maternal and fetal organs. Currently, there are few reliable tools to target the multi-functional placental SCTB for gene manipulation. In this study, we demonstrate the efficiency and specificity of the *SynbCre* transgenic line at deleting *Fpn1* from the SCTB in late gestation mouse placentas. Our data provide direct evidence of an essential role of placental *Fpn1* for fetal survival. Like *Fpn1*, many placental genes including *Tfrc* are considered essential due to the embryonic lethality in the whole-body KO models. Placental specific deletions of these genes using tools like *SynbCre* are needed to directly address their functional significance in supporting fetal growth. The *SynbCre* is uniquely valuable in studying SCTB gene functions *in vivo* and will facilitate the generation of mouse models of pregnancy complications and fetal abnormalities.

Materials and Methods

Animals

Wild-type (WT) 129S6/SvEvTac mice were obtained from Taconic Biosciences. *Fpn1*-floxed mice (129S-Slc40a1tm2Nca/J)(Donovan, Lima et al. 2005) were purchased from The Jackson Laboratory. A germline *Fpn1* KO allele was generated by crossing the *Fpn1* floxed mice with the GATA1 *Cre* line (129S.Cg-Tg(Gata1-cre)1Sho/MdfJ) (Mao, Fujiwara et al. 1999). Both the *Fpn1* floxed and KO alleles had been backcrossed to 129S6/SvEvTac for more than 10 generations. Enhanced Yellow Fluorescent Protein (YFP) reporter mice (B6.129X1-Gt(ROSA)26Sortm1(EYFP)Cos/J)(Srinivas, Watanabe et al. 2001) were a gift from Dr. Yuko Fujiwara (Boston Children's Hospital) and were originally purchased from the Jackson Laboratory. Unless otherwise stated, genotyping was performed using specific probes by the automated genotyping service at Transnetyx. Mice had ad libitum access to water and standard chow. All animal protocols were approved by the Institutional Animal Care and Use Committee at Boston Children's Hospital.

Generation of *SynbCre* transgenic mice

SynbCre mice were generated using a protocol modified from the Easi-CRISPR method (Quadros, Miura et al. 2017). Briefly, a single guide RNA (sgRNA) targeting the mouse *Synb* gene (ENSMUSG00000047977) was selected based on high on-target and off-target scores using the Benchling CRISPR design tool (https://www.benchling.com/crispr/). The sgRNA oligo (GACACCATTCCTACATAACA) was synthesized by Synthego. The presence of the sgRNA site in the *Synb* gene was verified in the FVB/NJ genome by PCR and Sanger sequencing (Genewiz LLC). A megamer single-stranded DNA (ssDNA) donor containing the sequence of the self-cleaving peptide porcine teschovirus-1 2A (P2A) and *Cre* inserted immediately before the stop codon of *Synb* was synthesized as the repair template by Integrated DNA Technologies. The donor ssDNA was injected into FVB/NJ zygotes along with the sgRNA and CAS9 protein (CP01, PNA Bio). Tail DNA was extracted from live offspring and screened for correct *Cre* insertions at the 5' and 3' junctions by PCR. *SynbCre* founders were bred to 129S6/SvEvTac *WT* mice to pass down the *Cre* transgene, and the *SynbCre* animals used in this study were backcrossed for at least 3 generations. Primers used in genomic PCR assays are provided in Table S1.

Time course and cell specificity of *SynbCre* in the placenta

To determine the time course of *SynbCre* expression, timed matings were set up between 129S6/SvEvTac males carrying *SynbCre* and *WT* females. Placentas were collected from E10.5 (the formation of the placenta) to E18.5 (end of gestation) (n=3-7 placentas from 1-2 dams/time point). RNA extraction and quantitative RT-PCR (qPCR) analysis were performed as described previously (Cao, Prado et al. 2021). Various organs were harvested from 2 *SynbCre* positive adult mice (6-10 weeks of age) to assess Cre expression in adult tissues. Transcript abundance of *Cre* was calculated by the $2(-\Delta\Delta CT)$ method, using *beta-actin (Actb)* as the housekeeping control and *SynbCre* positive placentas as the reference group. RNA samples in the same experiments were run in one batch on the same plate. Primers used in qPCR are included in Table S1.

Cell specificity and recombination activity of *SynbCre* were determined by crossing *SynbCre* to the YFP reporter line. Placentas were collected at E15.5, fixed in 4% paraformaldehyde, cryo-sectioned, and immunostained for YFP (ab13970; Abcam) alongside the SCTB marker connexin 26 (CX26) (71-0500; Invitrogen) using methods reported elsewhere (Cao and Fleming 2021).

Generation of placental *Fpn1* KO (pKO)

SynbCre was bred to *Fpn1* heterozygous animals to generate Cre-positive *Fpn1* heterozygous males (*Fpn1*$^{-/+}$*; SynbCre*). Conditional deletion of *Fpn1* in the placenta was achieved by crossing *Fpn1*$^{-/+}$*; SynbCre* males with homozygous *Fpn1 floxed* females (*Fpn1*$^{fl/fl}$). By introducing the *Fpn1 KO* allele in the male parent, this pairing strategy would reduce the risk of mosaicism due to ineffective *Cre*-mediated excision when there are two floxed alleles. This design also circumvented the use of parents carrying both *Cre* and *Fpn1 floxed* allele thus avoiding the impact of placental *Fpn1* deletion during embryogenesis of the parental generation.

During dissection, maternal decidua of the placenta was removed, and the fetal portion enriched for the labyrinth was divided into quadrants, processed for paraformaldehyde fixation or stored at -80°C for RNA and protein extractions as previously described (Cao, Prado et al. 2021). In most cases, an additional placental tissue was weighed and processed for non-heme iron determination. Sizes of the embryo and the placenta were measured as crown rump length (CRL) and the diameter of the placental disk. Embryos and placentas were separately genotyped for *Fpn1 floxed*, *KO*, *WT*, *Cre*, and the sex chromosome *Y*. Phenotyping comparisons were carried out between the pKO (*Fpn1*$^{fl/-}$; *SynbCre*) and the *Cre* negative control (*Fpn1*$^{fl/-}$). During the initial phase of pKO phenotyping, we performed cryo-sectioning and FPN1 immunofluorescence in placental tissues immediately (1-2 days) after dissection to confirm FPN1 protein deletion in the pKO. The consistency of placental FPN1 deletion and pale appearance in the pKO embryos provided us reassurance to remove this confirmatory step and save all the fixed placentas for paraffin embedding for better structure preservation and batched analysis of placentas from different litters.

A total of 15 pKO and 7 control placentas were collected from 5 different litters at E15.5. All 22 placentas were used for RNA extraction and analyzed for *Fpn1* transcript abundance by qPCR as an initial confirmation for *Fpn1* deletion. Sequences of primers used in qPCR are provided in Table S1. In three of the E15.5 litters, fetal liver (n=5 pKO and n=5 control) was collected for RNA extraction. Whole embryos (n=2 pKO and n=2 control) were fixed and processed for histology.

Placental tissue iron

Iron was extracted from placental tissues (n=13 pKO and n=5 control) in a trichloroacetic and hydrochloric acid mix at 65°C for 2 days. Non-heme iron concentrations in the extracts were determined by the bathophenanthroline quantification method as described previously (Torrance and Bothwell 1980, Cao, Prado et al. 2021).

Histology and immunofluorescence

Fixed placentas were embedded in paraffin and sectioned at 10 µm. General cellular morphology was assessed by hematoxylin and eosin staining. Cellular iron was visualized by Perl's Prussian Blue staining followed by signal enhancement with 3,3' diaminobenzidine tetrahydrochloride (DAB). Bright-field images were acquired using an Olympus BX50 microscope.

Immunofluorescence was performed using antibodies against FPN1 (MTP11-A; Alpha Diagnostic International), TFRC (13-6800; Invitrogen), FTL1 (HPA041602; Sigma-Aldrich), CX26 (71-0500; Invitrogen) and isolectin B4 (I32450; Thermofisher), as detailed elsewhere (Cao, Prado et al. 2021). At least two placentas of each genotype were stained in the same batch and imaged using the same settings with a Zeiss Observer D1 fluorescent microscope.

Western blotting

Protein extraction and western blotting were carried out as described before (Cao, Prado et al. 2021). A random sample of 11 placentas including 6 pKO and 5 controls were selected so they could be run on the same 12-well TruPAGE gel (Sigma-Aldrich) and analyzed in the same experiment. Primary antibodies used include: FPN1 (MTP11-A; Alpha Diagnostic International), TFRC (13-6800; Invitrogen), FTL1 (HPA041602; Sigma-Aldrich), FTH1 (4393S, Cell Signaling Technology), and ACTB (4970S, Cell Signaling Technology). Band intensities were quantified by Image Lab software (Bio-Rad Laboratories) and normalized to the intensity of ACTB in the same sample.

Placental RNA-sequencing

RNA-sequencing was performed in 6 pKO and 4 control male placentas. These placentas were from 4 litters at E15.5, each contributing 1 control and 1-2 pKO placentas. Only male placentas were used to avoid differential sequencing coverage of the sex chromosomes and the resulting distortion of non-sex genes in transcriptomic analysis. We chose the males because there were more matched male pKO and control placentas than female pairs at the time of RNA-sequencing. Analysis of all 22 male and female pKO and control placentas did not show significant gender differences in the degree of *Fpn1* deletion, placental genes, placental iron concentrations, or embryo phenotype. Male and female mouse placentas may have different transcriptomic responses to environmental stimuli such as maternal iron deficiency as we demonstrated in a previous study (Cao, Prado et al. 2021). However, we did not find gender differences in how the placental iron metabolic genes/proteins responded to maternal iron

deficiency and there were no transcriptomic differences (other than the sex specific genes) between male and female placentas at baseline. Nonetheless, it is critical to study and confirm key outcomes including placental and embryonic phenotype in both genders when using *Cre* deleters such as the *SynbCre.* RNA integrity was analyzed on an Agilent TapeStation 4200. The RNA integrity numbers (RIN) of the placental samples were greater than 8 and averaged 9.4.

Library construction and sequencing were performed by Genewiz, LLC, using NEBNext Ultra RNA Library Prep Kit and Illumina HiSeq 4000 with a 2 x 150-bp paired-end configuration. Bioinformatic analysis was carried out using a similar pipeline as described before (Cao, Prado et al. 2021). In short, reads were trimmed by Trimmomatic (v.0.36), aligned to the mouse reference genome (GRCm38.p6) by STAR aligner (v.2.5.2b), counted by featureCounts from the Subread package (v.1.5.2). Counts were used for exon usage analysis using the R package DEXSeq v.1.42.0 (Anders, Reyes et al. 2012). Differentially expressed genes (DEGs) were identified using DESeq2 package (v.1.32.0) (Love, Huber et al. 2014), when false discovery rate (FDR) adjusted P-values < 0.05. Multiple testing correction is a standard procedure in DEG analysis of RNA-sequencing data and the DESeq2 package implements the Benjamini-Hochberg algorithm by default to control the overall FDR in multiple tests of independent P values (Benjamini and Hochberg 1995, Love, Huber et al. 2014, Koch, Chiu et al. 2018). Gene ontology (GO) enrichment analysis was performed using the clusterProfiler package (v.4.0.5) (Yu, Wang et al. 2012). Pathways with FDR adjusted P-value < 0.05 were considered significant.

Statistical analysis

Statistical analyses (except for RNA-Sequencing) were performed in JMP 16.0 (SAS Institute). Differences between two samples were compared by Student's t-tests for normally distributed variables and by Wilcoxon rank sum tests for non-normally distributed variables. Pearson correlation was used to examine the relation between placental *Synb* and *Cre* mRNA expression. Unless otherwise stated, data were expressed as mean ± standard deviation (SD). Significance was defined as P-value < 0.05.

Author contributions

Chang Cao, Conceptualization, Methodology, Investigation, Writing - original draft, review, and editing. Mark D Fleming, Supervision, Writing - review and editing.

Acknowledgments

We are grateful to Dr. Chen Wu, Dr. Joel Lawitt, and Jennifer Mark at the Transgenic Core of Beth Israel Deaconess Medical Center for their expertise and efficiency in generating the *SynbCre* mouse. We thank Dr. Liang Sun at the Boston Children's Hospital for his advice on RNA-sequencing analysis. We extend our gratitude to the Bioinformatics Core at Harvard T.H. Chan School for providing training courses on RNA-sequencing data processing and analysis. We are indebted to the staff at Animal Resources of Children's Hospital at Boston Children's Hospital for keeping the animal facility running through the COVID-19 pandemic, which allowed this research to come to fruition.

Funding

Funding for this study came from the Allen Foundation, Inc and Children's Hospital Pathology Foundation, Inc.

Declaration of Interests

The authors declare no conflicts of interest.

Data availability

The RNA-sequencing data have been deposited in the Gene Accession Omnibus under accession ID GSE206109. Investigators interested in the *SynbCre* mouse used in the study should contact Dr. Mark Fleming at Boston Children's Hospital.

References

Anders, S., A. Reyes and W. Huber (2012). "Detecting differential usage of exons from RNA-seq data." Genome Research **22**(10): 2008-2017.

Benjamini, Y. and Y. Hochberg (1995). "Controlling the False Discovery Rate: A Practical and Powerful Approach to Multiple Testing." Journal of the Royal Statistical Society: Series B (Methodological) **57**(1): 289-300.

Calzonetti, T., L. Stevenson and J. Rossant (1995). "A novel regulatory region is required for trophoblast-specific transcription in transgenic mice." Dev Biol **171**(2): 615-626.

Cao, C. and M. D. Fleming (2021). "Localization and Kinetics of the Transferrin-Dependent Iron Transport Machinery in the Mouse Placenta." Current Developments in Nutrition **5**(4).

Cao, C., M. A. Prado, L. Sun, S. Rockowitz, P. Sliz, J. A. Paulo, D. Finley and M. D. Fleming (2021). "Maternal Iron Deficiency Modulates Placental Transcriptome and Proteome in Mid-Gestation of Mouse Pregnancy." The Journal of Nutrition **151**(5): 1073-1083.

Donovan, A., C. A. Lima, J. L. Pinkus, G. S. Pinkus, L. I. Zon, S. Robine and N. C. Andrews (2005). "The iron exporter ferroportin/Slc40a1 is essential for iron homeostasis." Cell Metab **1**(3): 191-200.

Dupressoir, A., C. Vernochet, F. Harper, J. Guégan, P. Dessen, G. Pierron and T. Heidmann (2011). "A pair of co-opted retroviral envelope syncytin genes is required for formation of the two-layered murine placental syncytiotrophoblast." Proceedings of the National Academy of Sciences **108**(46): E1164-E1173.

Gálvez-Peralta, M., L. He, L. F. Jorge-Nebert, B. Wang, M. L. Miller, B. L. Eppert, S. Afton and D. W. Nebert (2012). "ZIP8 zinc transporter: indispensable role for both multiple-organ organogenesis and hematopoiesis in utero." PLoS One **7**(5): e36055.

Gunshin, H., Y. Fujiwara, A. O. Custodio, C. DiRenzo, S. Robine and N. C. Andrews (2005). "Slc11a2 is required for intestinal iron absorption and erythropoiesis but dispensable in placenta and liver." The Journal of Clinical Investigation **115**(5): 1258-1266.

Guttmacher, A. E., Y. T. Maddox and C. Y. Spong (2014). "The Human Placenta Project: placental structure, development, and function in real time." Placenta **35**(5): 303-304.

Hemberger, M., C. W. Hanna and W. Dean (2020). "Mechanisms of early placental development in mouse and humans." Nature Reviews Genetics **21**(1): 27-43.

Koch, C. M., S. F. Chiu, M. Akbarpour, A. Bharat, K. M. Ridge, E. T. Bartom and D. R. Winter (2018). "A Beginner's Guide to Analysis of RNA Sequencing Data." American Journal of Respiratory Cell and Molecular Biology **59**(2): 145-157.

Li, H., H.-K. Sung, D. Qu, A. Nagy and S. L. Adamson (2014). 26 - Conditional Gene Deletion in the Placenta Using the Cre-loxP System. The Guide to Investigation of Mouse Pregnancy. B. A. Croy, A. T. Yamada, F. J. DeMayo and S. L. Adamson. Boston, Academic Press**:** 309-313.

Love, M. I., W. Huber and S. Anders (2014). "Moderated estimation of fold change and dispersion for RNA-seq data with DESeq2." Genome Biology **15**(12): 550.

Mao, X., Y. Fujiwara and S. H. Orkin (1999). "Improved reporter strain for monitoring Cre recombinase-mediated DNA excisions in mice." Proc Natl Acad Sci U S A **96**(9): 5037-5042.

Mok, H., M. Mendoza, J. T. Prchal, P. Balogh and A. Schumacher (2004). "Dysregulation of ferroportin 1 interferes with spleen organogenesis in polycythaemia mice." Development **131**(19): 4871-4881.

Nadeau, V. and J. Charron (2014). "Essential role of the ERK/MAPK pathway in blood-placental barrier formation." Development **141**(14): 2825-2837.

Nadeau, V., S. Guillemette, L. F. Bélanger, O. Jacob, S. Roy and J. Charron (2009). "Map2k1 and Map2k2 genes contribute to the normal development of syncytiotrophoblasts during placentation." Development **136**(8): 1363-1374.

Nemeth, E. and T. Ganz (2021). "Hepcidin-Ferroportin Interaction Controls Systemic Iron Homeostasis." International Journal of Molecular Sciences **22**(12): 6493.

Quadros, R. M., H. Miura, D. W. Harms, H. Akatsuka, T. Sato, T. Aida, R. Redder, G. P. Richardson, Y. Inagaki, D. Sakai, S. M. Buckley, P. Seshacharyulu, S. K. Batra, M. A. Behlke, S. A. Zeiner, A. M. Jacobi, Y. Izu, W. B. Thoreson, L. D. Urness, S. L. Mansour, M. Ohtsuka and C. B. Gurumurthy (2017). "Easi-CRISPR: a robust method for one-step generation of mice carrying conditional and insertion alleles using long ssDNA donors and CRISPR ribonucleoproteins." Genome Biology **18**(1): 92.

Renaud, S. J., M. A. Karim Rumi and M. J. Soares (2011). "Review: Genetic manipulation of the rodent placenta." Placenta **32 Suppl 2**(Suppl 2): S130-S135.

Roberts, R. M., J. A. Green and L. C. Schulz (2016). "The evolution of the placenta." Reproduction (Cambridge, England) **152**(5): R179-R189.

Sadovsky, Y., V. L. Clifton and G. J. Burton (2014). "Invigorating placental research through the "Human Placenta Project"." Placenta **35**(8): 527.

Sangkhae, V., A. L. Fisher, S. Wong, M. D. Koenig, L. Tussing-Humphreys, A. Chu, M. Lelić, T. Ganz and E. Nemeth (2021). "Effects of maternal iron status on placental and fetal iron homeostasis." The Journal of Clinical Investigation **130**(2).

Simmons, D. G., A. L. Fortier and J. C. Cross (2007). "Diverse subtypes and developmental origins of trophoblast giant cells in the mouse placenta." Developmental Biology **304**(2): 567-578.

Srinivas, S., T. Watanabe, C. S. Lin, C. M. William, Y. Tanabe, T. M. Jessell and F. Costantini (2001). "Cre reporter strains produced by targeted insertion of EYFP and ECFP into the ROSA26 locus." BMC Dev Biol **1**: 4.

Torrance, J. D. and T. H. Bothwell (1980). Tissue iron stores. Methods in Haematology. J. D. Cook. New York, Churchill Livingstone**:** 90-115.

Watson, E. D. and J. C. Cross (2005). "Development of structures and transport functions in the mouse placenta." Physiology (Bethesda) **20**: 180-193.

Wenzel, P. L. and G. Leone (2007). "Expression of Cre recombinase in early diploid trophoblast cells of the mouse placenta." genesis **45**(3): 129-134.

Yu, G., L. G. Wang, Y. Han and Q. Y. He (2012). "clusterProfiler: an R package for comparing biological themes among gene clusters." Omics **16**(5): 284-287.

Figures

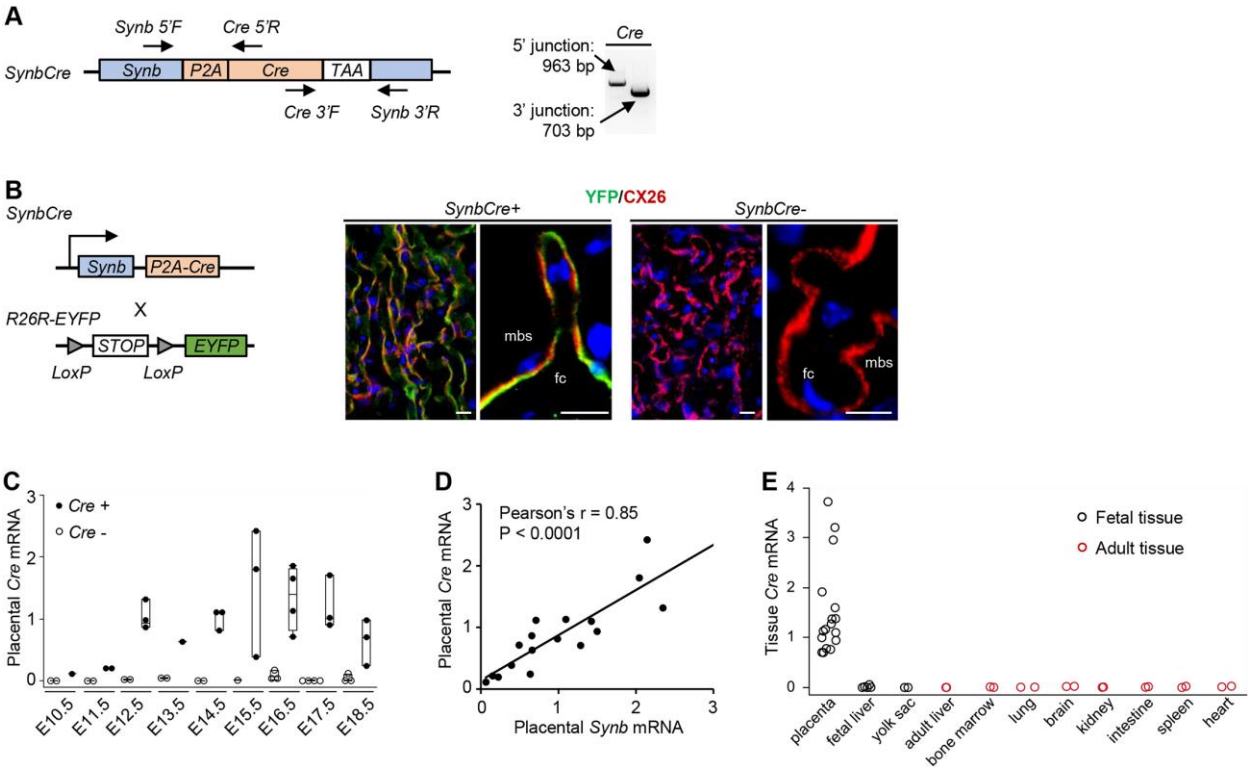

Fig. 1. Generation and characterization of the *SynbCre* mouse. (A) Design of *SynbCre* knock-in allele. P2A-Cre was inserted immediately before the stop codon (TAA) of *Synb*. Primer locations for 5' and 3' junction PCRs are shown along with expected amplicon sizes. (B) *SynbCre* induced YFP expression in the mouse placenta. Left: *SynbCre* was bred to the R26R-EYFP reporter allele and resulted in excision of the *LoxP* flanked STOP sequence and subsequent expression of YFP in *Cre* expressing cells. Right: Immunofluorescence of YFP (green) and SCTB marker CX26 (red) in *SynbCre* positive and negative placentas at E15.5. Abbreviations: mbs, maternal blood space; fc, fetal circulation. Scale bars = 15 μm (C) *SynbCre* mRNA expression in mouse placentas from E10.5 to E18.5 (n=3-7/time point). Placentas were collected from 1-2 dams/time point. *SynbCre* positive placentas are represented by full circles and *SynbCre* negative controls are represented by empty circles. (D) Correlation between *Synb* and *Cre* mRNA expression in *SynbCre* positive placentas (n=17). Pearson's correlation = 0.85, $P < 0.0001$. (E) *Cre* mRNA expression in *SynbCre* carrying tissues including placentas (n=17), fetal liver (n=5), yolk sac (n=3), and adult tissues (n=2). Black circles represent fetal tissues and red circles represent adult tissues.

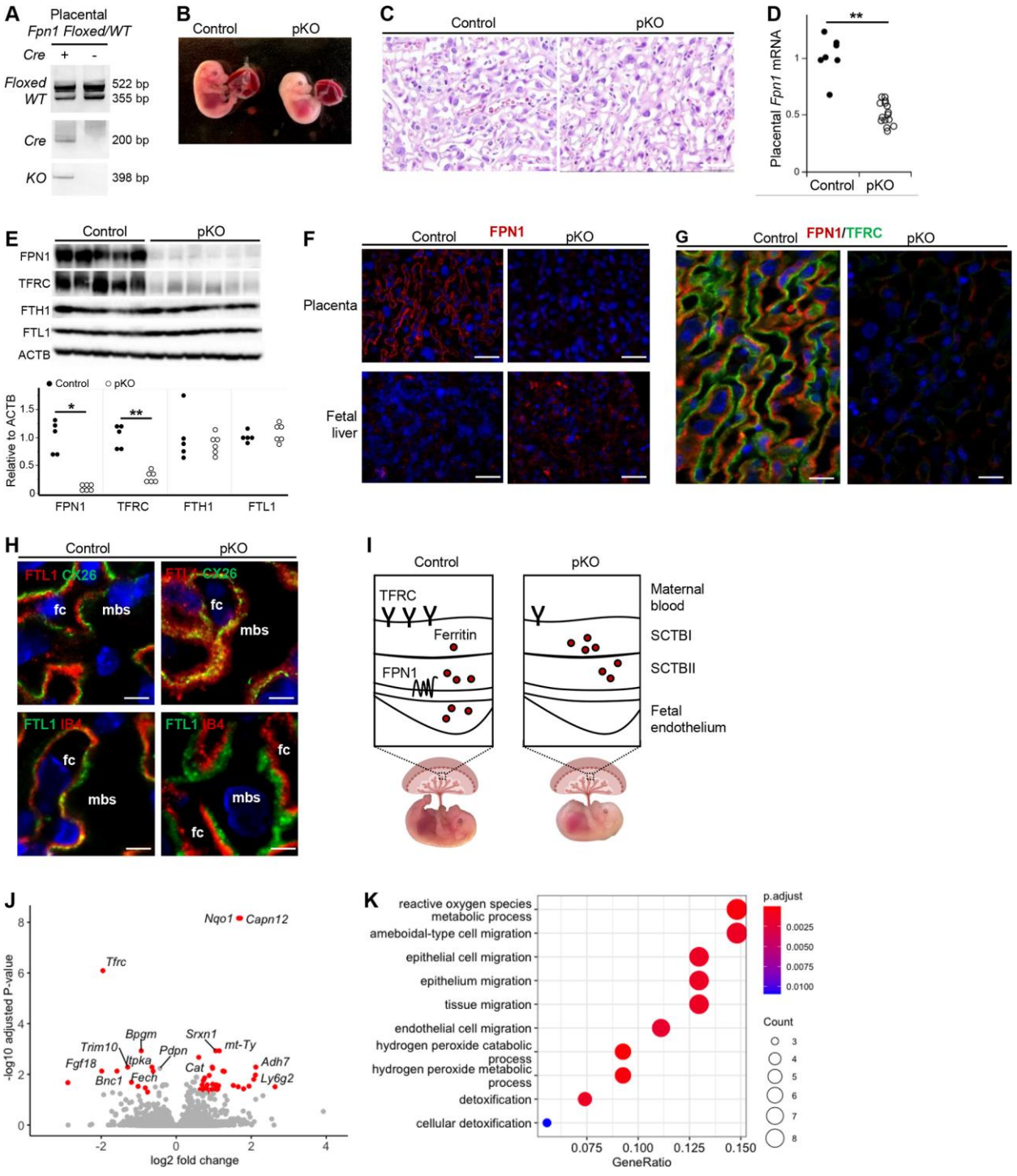

Fig. 2. Effects of placental *Fpn1* deletion by *SynbCre*. (A) Genotyping PCRs of *SynbCre* positive and negative placentas carrying the same inherited parental *Fpn1* alleles (one floxed and one *WT*). (B) Representative image of placental *Fpn1* KO and the control embryos at E15.5. (C) H and E staining of control and pKO placentas. Scale bar = 100 μm. (D) Relative expression

of *Fpn1* mRNA in control (n=7) and pKO placentas (n=15). **, P < 0.001. (E) Western blots of iron metabolic proteins in the control (n=5) and pKO placentas (n=6). Bottom: Densitometric analysis of protein quantification between control and pKO placentas. Control placentas are shown as full circles and pKO placentas are represented as empty circles. *, P < 0.01 **, P < 0.001. (F) Immunofluorescence of FPN1 in control, pKO placentas, and fetal liver. Scale bar = 50 μm. (G) Immunofluorescence of FPN1 (red) and TFRC (green) in control and pKO placentas. Scale bar = 20 μm. (H) Ferritin distribution in the labyrinth cell layers in control and pKO placentas. Ferritin light chain (FTL1) is co-stained with SCTB marker CX26 (Top panel) and the endothelium marker IB4 (Bottom panel). mbs, maternal blood space; fc, fetal circulation. Scale bar = 10 μm. (I) Graphic summary of the effects of *Fpn1* deletion in late gestation placenta on the placenta and the embryo. pKO placentas have reduced TFRC and ferritin accumulation in the SCTB. pKO embryos are pale and small and die before birth. (J) Volcano plot of differentially expressed gene (DEG) analysis results of control (n=4) and pKO (n=6) placentas. DEGs are shown in red and non-significant genes are in gray. The twenty genes with the lowest FDR adjusted P values are labeled with the gene names. (K) Dot plot of the ten most significantly enriched gene ontology (GO) terms in the DEGs. The size of the dot corresponds to the number of genes associated with the GO term. The color of the dot represents the FDR adjusted P-value of the enrichment GO.

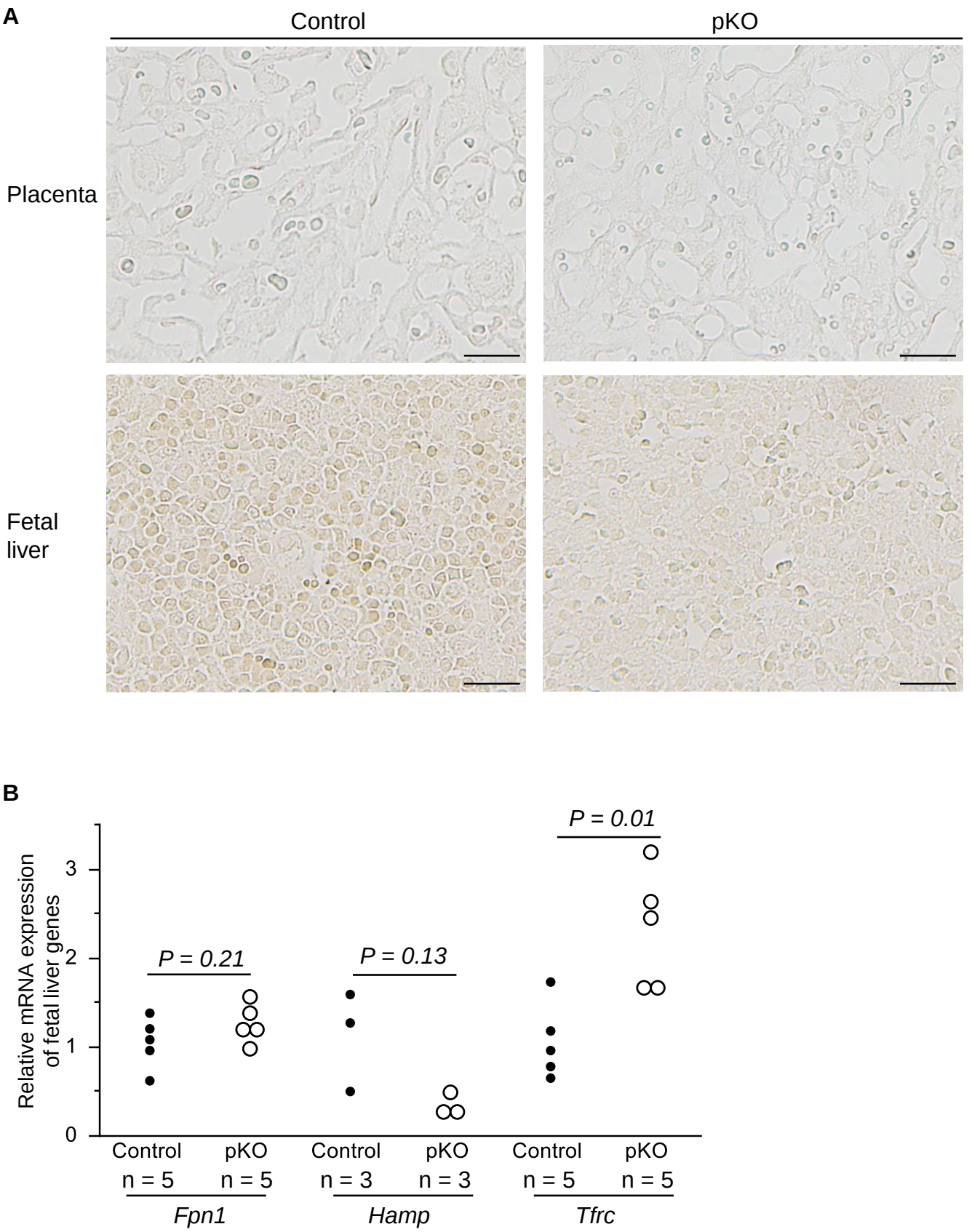

Fig. S1. Iron status indicators in control and pKO embryos at E15.5. (A) Perls-DAB iron stain in control and pKO placentas and fetal livers; Scale bar = 10 μm. (B) Transcript expression of iron genes in fetal liver of control and pKO embryos.

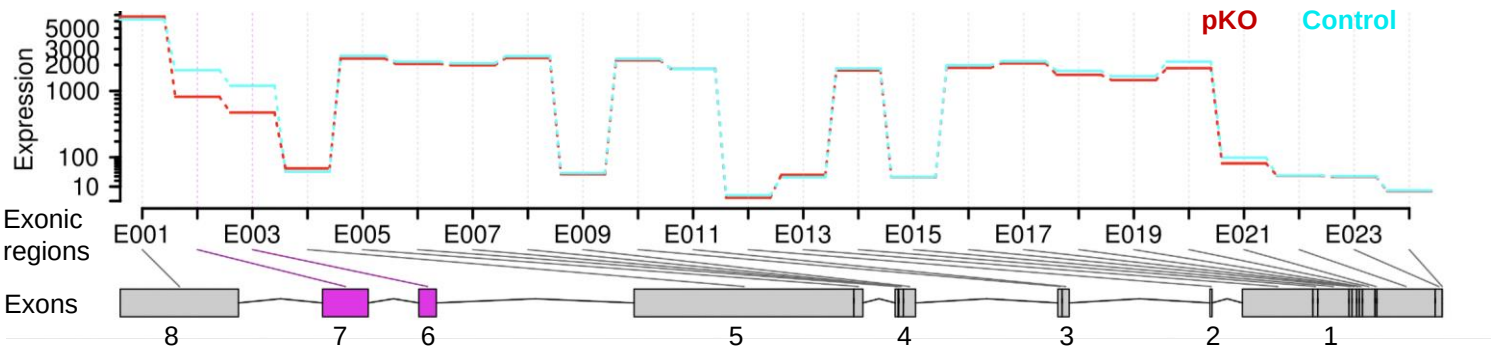

Fig. S2. Expression of Fpn1 exons in pKO and control placentas. Exons 6 and 7 (in magenta) had significantly lower usage in pKO placentas than the controls.

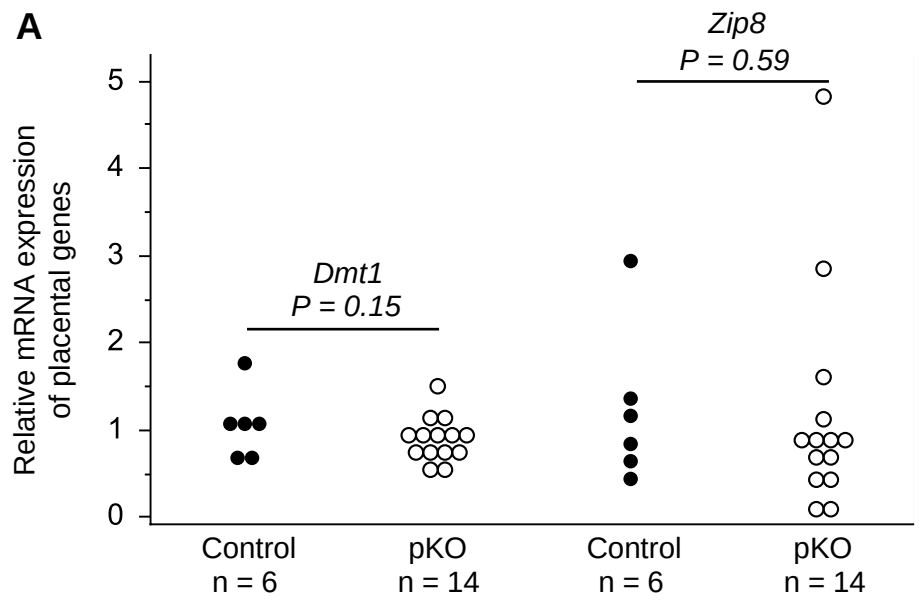

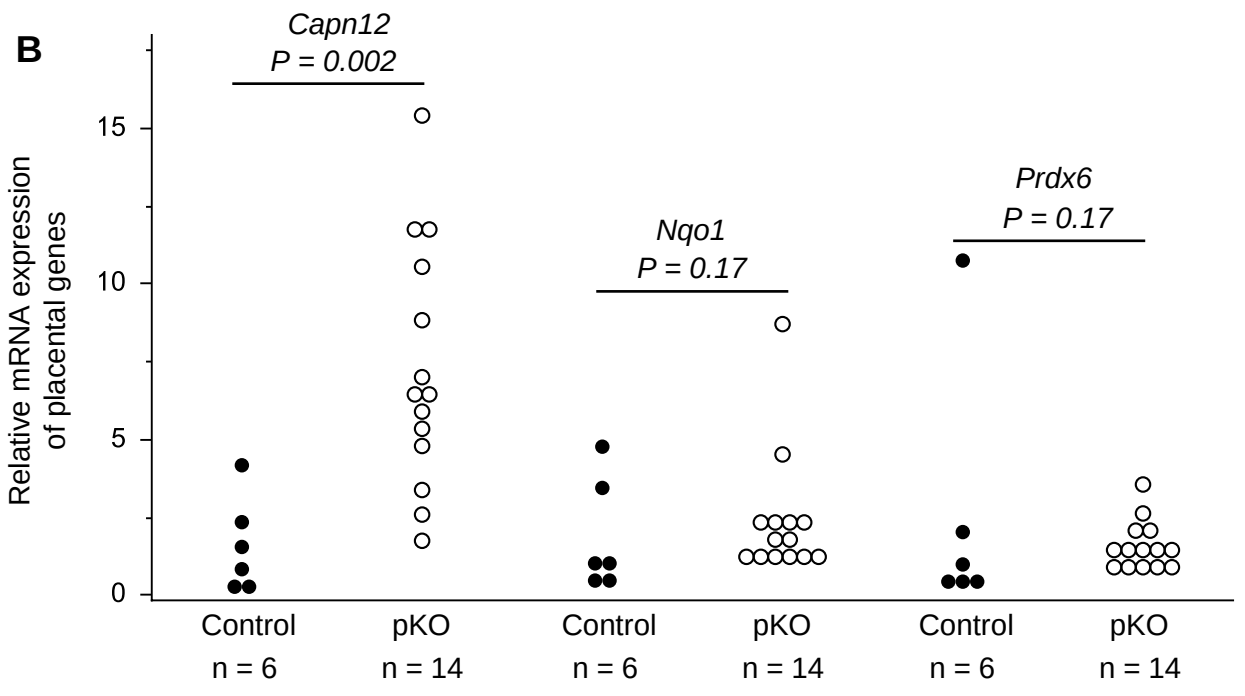

Fig. S3. qPCR of selected iron transporter genes (A) and oxidative stress genes (B) in pKO and control placentas (n=20; from 4 different litters).

Table S1. Primers used in genotyping and quantitative PCR (qPCR)

	Forward	Reverse
Genotyping PCR		
Fpn1 WT/Floxed	CTACACGTGCTCTCTTGAGAT	GGTTAAACTGCTTCAAAGG
Fpn1 KO	CTACACGTGCTCTCTTGAGAT	CCTCATATGTGAGTCAAAGTATAG
SynbCre insert 5’	AACGAGCATCTGAACTCGGC	CGCCGCATAACCAGTGAAAC
SynbCre insert 3’	ACATGCTTCATCGTCGGTCC	TGTCTGAGATGGGGGCTACT
Cre	CGTATAGCCGAAATTGCCAG	CAAAACAGGTAGTTATTCGG
qPCR		
Tfrc	GTGGAGTATCACTTCCTGTCGC	CCCCAGAAGATATGTCGGAAAGG
Fpn1	CCCATAGTCTCTGTCAGCCTGC	CCGTCAAATCAAAGGACCAAA
Actb	ACCCACACTGTGCCCATCTA	CACGCTCGGTCAGGATCTTC
Hamp	CTGAGCAGCACCACCTATCTC	TGGCTCTAGGCTATGTTTTGC
Synb	CCACCACCCATACGTTCAAA	GGTTATAGCAGGTGCCGAAG
Cre	CCTGTTTTGCACGTTCACCG	ATGCTTCTGTCCGTTTGCCG
Slc11a2	TCCTCATCACCATCGCAGACACTT	TCCAAACGTGAGGGCCATGATAGT
Slc39a8	CTCGCCTTCAGTGAGGATGT	GCTTTGCGTTGTGCTTTCTT
Nqo1	AGGATGGGAGGTACTCGAATC	AGGCGTCCTTCCTTATATGCTA
Prdx6	CGCCAGAGTTTGCCAAGAG	TCCGTGGGTGTTTCACCATTG
Capn12	GAGGCTTCAACTCCGGTGG	GTTGCGCTGGATGAGTGACA

Table S2. Differentially expressed genes in pKO placentas compared to the controls identified by RNA-sequencing

Click here to download Table S2

Table S3. Gene ontology analysis of biological processes enriched in the differentially expressed genes in pKO placentas compared to the control placentas

Click here to download Table S3